JACS
JOURNAL OF THE AMERICAN CHEMICAL SOCIETY
pubs.acs.org/JACS
Article

Metastability of Protein Solution Structures in the Absence of a Solvent: Rugged Energy Landscape and Glass-like Behavior

Tyler. C. Cropley, Fanny. C. Liu, Mengqi Chai, Matthew F. Bush, and Christian Bleiholder*

Cite This: https://doi.org/10.1021/jacs.3c12892
Read Online
ACCESS | Metrics & More | Article Recommendations | Supporting Information

ABSTRACT: Native ion mobility/mass spectrometry is well-poised to structurally screen proteomes but characterizes protein structures in the absence of a solvent. This raises long-standing unanswered questions about the biological significance of protein structures identified through ion mobility/mass spectrometry. Using newly developed computational and experimental ion mobility/ion mobility/mass spectrometry methods, we investigate the unfolding of the protein ubiquitin in a solvent-free environment. Our data suggest that the folded, solvent-free ubiquitin observed by ion mobility/mass spectrometry exists in a largely native fold with an intact β-grasp motif and α-helix. The ensemble of folded, solvent-free ubiquitin ions can be partitioned into kinetically stable subpopulations that appear to correspond to the structural heterogeneity of ubiquitin in solution. Time-resolved ion mobility/ion mobility/mass spectrometry measurements show that folded, solvent-free ubiquitin exhibits a strongly stretched-exponential time dependence, which simulations trace to a rugged energy landscape with kinetic traps. Unfolding rate constants are estimated to be approximately 800 to 20,000 times smaller than in the presence of water, effectively quenching the unfolding process on the time scale of typical ion mobility/mass spectrometry measurements. Our proposed unfolding pathway of solvent-free ubiquitin shares substantial characteristics with that established for the presence of solvent, including a polarized transition state with significant native content in the N-terminal β-hairpin and α-helix. Our experimental and computational data suggest that (1) the energy landscape governing the motions of folded, solvent-free proteins is rugged in analogy to that of glassy systems; (2) large-scale protein motions may at least partially be determined by the amino acid sequence of a polypeptide chain; and (3) solvent facilitates, rather than controls, protein motions.

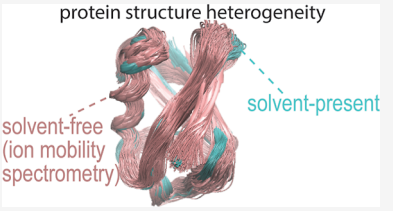

INTRODUCTION

Proteins and their complexes derive their biological function from the structures that they adopt and the motions through which they interconvert. Although early models viewed proteins as static entities,[1] it is now widely recognized that protein function is best described in terms of an energy landscape comprising a hierarchy of conformational states and transitions between them at various scales of length, time, and energy.[2−4]

The dynamic nature of protein function takes on increased complexity in the context of cellular processes, which depend on the collective action of all proteins ("proteome"). Mechanisms such as post-translational modifications of proteins may alter protein interaction networks and trigger disease phenotypes.[5] Mass spectrometry methods are well-suited to handle the heterogeneity arising from proteoforms or assembly steady-states and enable systematic measurements of proteomes.[6] When combined with ion mobility spectrometry (IM/MS), these methods have shown great promise in studying heterogeneous protein systems, from lipid-bound membrane proteins[7] to structurally heterogeneous glycoproteins[8] and disorder−order transitions of amyloid assemblies implicated in neurodegenerative diseases.[9,10]

However, native IM/MS characterizes protein structures without a solvent. Because solvent molecules stabilize proteins in their native state,[11] proteins may adopt non-native conformations during IM/MS analysis. For example, proteins adopt non-native, kinetically stable structures upon energetic activation,[12,13] and the peaks in native IM/MS measurements are usually broader than expected for a single conformer.[14,15] Further, functionally important protein motions are generally thought to be driven by solvent dynamics.[16,17] These considerations underline that the lack of solvent raises long-standing, unanswered questions about the extent to which IM/MS reveals biologically relevant protein structures.[18]

Early studies noted that organic solvents promote protein denaturation but simultaneously reduce denaturation rates, so native protein conformations become kinetically trapped.[19] There is ample experimental evidence that electrospray ionization produces protein ions that retain aspects of their native structures.[18,20−24] The questions we are interested in are how closely these solvent-free protein ions reflect the native state and to what extent solvent regulates the protein (un)folding pathway.

Received: November 16, 2023
Revised: March 29, 2024
Accepted: March 29, 2024

Protein denaturation upon removal of the solvent is represented by the simplified free energy profiles in Figure 1.

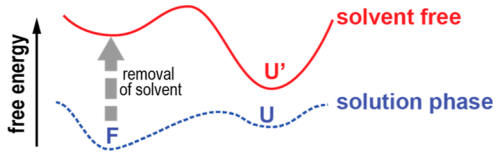

Figure 1. Simplified free-energy profiles describing protein folding in the presence (blue dashed trace) and absence (red solid trace) of a solvent. In the presence of solvent, equilibrium exists between the folded (native) state ***F*** and the unfolded state ***U***. Removal of solvent shifts the barrier and free energy profile along the unfolding coordinate and renders the folded state less stable than the unfolded state ***U′***. The consequence is a spontaneous relaxation of a folded solvent-free protein toward the unfolded state ***U′***. We discuss the relationship between the solvent-free and solvent-present energy landscapes.

In the presence of a solvent, equilibrium exists between a folded (native) state of a protein and an unfolded (non-native) state. In the absence of a solvent, folded protein structures are typically metastable but spontaneously unfold if given enough time and energy.[21−23,25−31] This suggests that the removal of solvent shifts the barrier and free energy profile along the unfolding coordinate, making the folded state less stable than the unfolded (denatured) state.

The origins of the barriers in the solvent-free environment and strategies to increase them remain incompletely understood, despite significant efforts. For example, the complexation of charged residues on the protein surface by residual solvent,[32] salts,[33] or crown ethers[34,35] has been proposed to prevent destabilizing interactions with the protein backbone. However, wild-type exoglycanase exhibits gas-phase barriers comparable to variants that lack charged residues.[36] Further, the stability of green fluorescent protein variants in the solvent-free environment appears to increase with the number of charged residues.[36] Moreover, the contributions of entropic or enthalpic components to the energy barriers remain underexplored, nor is it established how closely the initially formed, metastable structures correspond to the protein's native state.

In the presence of solvent, several protein folding scenarios have been associated with different free energy landscapes.[37] The primary determinant for these free energy landscapes is the interplay between enthalpic stabilization by native noncovalent contacts and changes in the configurational entropy during folding.[3,4] The position of the energy barrier on the folding coordinate determines the nativeness of the transition state ensemble,[38−40] which can be polarized with native structure present only in a subset of the protein. Additionally, scenarios have been discussed with rugged energy landscapes[37,41] and protein motions controlled by solvent fluctuations.[16,17,42,43]

Here, we characterize the unfolding of solvent-free ubiquitin by newly developed computational and experimental trapped ion mobility/trapped ion mobility/mass spectrometry (tandem-TIMS/MS) methods.[29,44] These methods allow us to partition solvent-free ubiquitin into subpopulations with different structures and characterize their time- and energy-resolved unfolding pathways. We selected bovine ubiquitin, a 76-residue globular protein, as a prototype because experimental and computational approaches have extensively characterized its solution-phase structure and dynamics.[39,45−55] The native state of ubiquitin is stable under a broad range of solution conditions[51] and shows functionally relevant structural heterogeneity in the ∼50 μs time scale regime.[49] Hence, ubiquitin is simple enough that unfolding in the absence of a solvent can be rigorously studied using our methods and compared with that established in the presence of a solvent.

MATERIALS AND METHODS

Materials and Sample Preparation. Chicken egg white lysozyme, bovine ubiquitin, ammonium acetate, and LC/MS grade water were obtained from Sigma-Aldrich (St. Louis, MO). Ubiquitin was desalted using a 3 kDa Amicon ultra centrifugal filter (Millipore Sigma, Burlington, MA) and diluted into LC/MS grade water to a concentration of 5 μM with aqueous 1% by volume acetic acid (pH 3.5). Lysozyme was desalted and diluted in 200 mM aqueous ammonium acetate (pH 6.5) to a final concentration of 5 μM.

Tandem-TIMS/MS Measurements. A full description of the experimental settings is given in Section S1 (Supporting Information). Briefly, ion mobility measurements were performed on a tandem-trapped IMS-QqTOF instrument (tandem-TIMS/MS, see Figure S1, Supporting Information) constructed[44] from the coupling of two independently controlled and differentially pumped prototype TIMS[56,57] devices to a QqTOF mass spectrometer. Samples were infused into the electrospray ionization (ESI) source in the positive ion mode through a gastight syringe (Hamilton, 250 μL) at a flow rate of 180 μL/h. The ability of this tandem-TIMS/MS instrument for soft, native-like measurements of proteins, protein complexes, and weakly bound peptide assemblies has been extensively demonstrated.[29,44,58−63] Ions produced from ESI are mobility-separated in TIMS-1. Following elution from TIMS-1, ions can be mobility-selected by timing a gating voltage in the interface region, as described in Figure S1 and elsewhere.[29,44,61] Comparing ion mobilities with TIMS-2 in "transmission mode" to those recorded in "separation mode" reveals if protein structures isomerize on the time scale of the separation process (Section S5, Supporting Information).[44,61] Mobility-selected subpopulations can be collisionally activated for collision-induced unfolding (CIU) measurements by dc-only electric fields between aperture-2 and deflector-2 (see Figure S1).[29,44,61,62,64] Time-resolved measurements can further be carried out by holding the trapping potential in the TIMS-2 constant for up to ∼21 s, as described.[44,65] Subsequently, ions are mobility-separated in TIMS-2. Ion mobilities and collision cross sections were calibrated as described[66−68] using perfluorophosphazenes contained in Agilent ESI tuning mix using reported reduced ion mobilities.[67,69] The error of the calibrated cross sections is typically less than 1%.[67,70] Nitrogen buffer gas was used for all ion mobility measurements.

Computational Details on SRA and PSA Calculations. Structure relaxation approximation (SRA) calculations were carried out as described.[29] Briefly, an ensemble of all-atom protein solution structures is (de)protonated to the desired charge state(s), and short gas-phase molecular dynamics (MD) simulations are separately carried out for each protein structure using GROMACS[71] version 4.5.7 in conjunction with the OPLS/AA[72] force field as described.[29] The charge states observed in the experiment were attained by (de)protonating solvent-accessible acidic and basic residues, as described.[29] To simulate the time-dependent unfolding of ubiquitin, we propagated each of the >1000 ubiquitin structures from the conformational ensemble for 3 μs at 450 K and stored snapshots for further analysis every 2 ns. To probe temperature dependence, analogous simulations were conducted at 500 K. Overall, roughly 4,000,000 collision cross sections were computed using our projection superposition approximation (PSA)[73] for nitrogen gas.[74] More details are found in Section S6 (Supporting Information).

RESULTS AND DISCUSSION

Solvent-Free, Compact Ubiquitin Subpopulations Reflect the Structural Heterogeneity of the Native State. The native state of ubiquitin is stable across various solution conditions.[51,54,55] Charge states 6+ to 8+ predominate the tandem-TIMS/MS spectra of bovine ubiquitin electrosprayed from aqueous solution at pH 3.5 (Figure 2), where its

https://doi.org/10.1021/jacs.3c12892
J. Am. Chem. Soc. XXXX, XXX, XXX−XXX

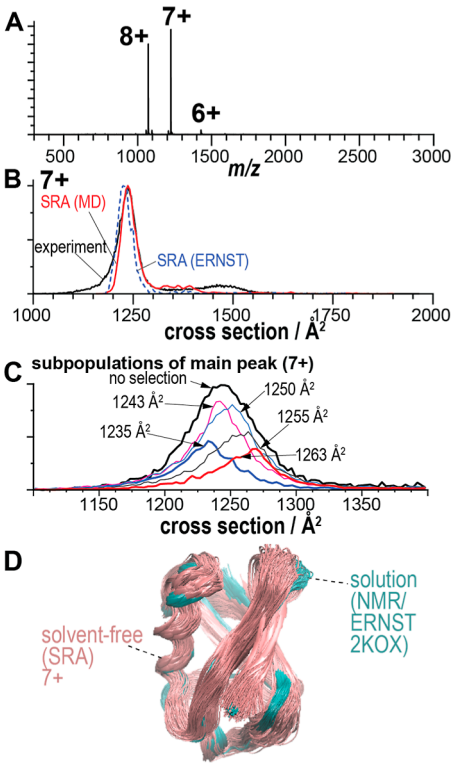

Figure 2. Solvent-free ubiquitin partitions into subpopulations that are consistent with the solution-phase conformational heterogeneity. (A) Charge states 6+ to 8+ predominate the mass spectrum of bovine ubiquitin electrosprayed from an aqueous solution at pH 3.5. (B) Ion mobility spectrum for charge state 7+ shows a dominant compact feature (black trace). Ion mobility spectra computed with our SRA method for the MD and ERNST ensembles (red traces and blue dashes, respectively) show a main, compact feature consistent with the experimental features. (C) Partitioning of the broad, compact feature (black trace) into a set of ubiquitin subpopulations (colored traces) with different collision cross sections that do not equilibrate on the ~100– ~200 ms time scale of the tandem-TIMS/MS experiments. All cross-sections were recorded in nitrogen buffer gas. (D) Comparison between the NMR-refined ubiquitin solution ensemble and the computed ensemble for solvent-free ubiquitin (SRA). Residues 72–76 have been omitted for clarity.

native state prevails. In line with prior literature,[29,74−76] the corresponding ion mobility spectra show a main compact feature with collision cross sections centered at 1186 Å^2 (6+), 1237 Å^2 (7+), and 1275 Å^2 (8+), respectively (see Figures 2, S2, and Table S1 in the Supporting Information). The full width at half-maxima of the dominant, compact peaks range from 44 to 66 Å^2, which are significantly broader than expected from the instrumental resolving power and indicate unresolved conformers. Consistent with prior literature,[77] the broad features can be partitioned into a set of subpopulations with different collision cross sections that do not appear to equilibrate on the ~100 ms time scale of the tandem-TIMS/MS experiments (Figure 2C and Section S5, Supporting Information). This means that these subpopulations retain structural differences on the ~100 ms measurement time scale. These results echo prior reports,[21,27,77] showing metastability of protein subpopulations in IM/MS.

To interpret the structure of ubiquitin in the solvent-free environment, we compared the experimental spectra to theoretical spectra computed using our SRA (see Figures 2 and S2 in the Supporting Information).[29,62] The SRA computes ion mobility spectra from an ensemble of protein solution structures by simulating the structural relaxation process that the protein undergoes in the absence of a solvent. For comparison to the experiment, we computed SRA spectra for charge states 6+ to 8+ from two reported solution ensembles for ubiquitin: For one, a set of 1500 structures from a 600 ns explicit-solvent all-atom MD simulation that was used in our original description of the SRA method.[29] Second, a set of 648 ubiquitin structures was refined against NMR data using the ensemble refinement for native proteins using a single alignment tensor (ERNST) approach (PDB code 2KOX).[78] Figures 2 and S2 (Supporting Information) show that the SRA spectra computed from both ensembles agree strongly with the experimental data for charge states 6+ to 8+. We emphasize that the computed ion mobility spectra reproduce the centers and relative widths of the dominant, compact peaks in the experimental spectra to within ~1 to ~2%, respectively (see Table S1, Supporting Information, for details), indicating a fraction of native contacts $Q \sim 0.9$ for the compact feature of charge states 6+ to 8+ with respect to the crystal structure (PDB code 1UBQ).[48] Figure 2D compares the structures computed for charge state 7+ (solvent-free, SRA) to the solution-phase ERNST ensemble,[78] underscoring the structural similarity between the solvent-free subpopulations and the ubiquitin solution ensemble as probed by NMR. These results indicate that the ubiquitin subpopulations in the absence of a solvent are consistent with the range of ubiquitin structures sampled in the presence of solvent. This interpretation mirrors variable-temperature IM/MS experiments that reported on 10 native conformations of chymotrypsin inhibitor 2 (CI2) from deconvolving broad peaks of ion mobility spectra with Gaussian functions.[79]

Solvent-Free Ubiquitin Subpopulations Originate from Distinct Solution-Phase Precursors. If the compact, solvent-free subpopulations of ubiquitin indeed reflect the structural heterogeneity of ubiquitin in solution, then they must not stem from different degrees of unfolding of a shared solution-phase precursor structure. This proposition can be experimentally tested by mild energetic activation (CIU): If the subpopulations originated from the same precursor structure and were formed by mild[20,80] energetic activation during ionization and desolvation, then they should isomerize upon mild collisional activation after elution from TIMS-1.

Hence, we selected five distinct ubiquitin subpopulations after elution from TIMS-1 (centered at 1231, 1241, 1246, 1255, and 1261 Å^2, respectively, see Table S2, Supporting Information), collisionally activated the selected subpopulations by an applied electric field, and measured the cross sections of the activated subpopulations in TIMS-2. The spectra reveal that the subpopulations unfold in two steps *via* a partially unfolded feature centered at ~1520 Å^2 before an unfolded species at ~1830 Å^2 emerges (Figure S4, Supporting Information). Figure 3 shows that more than 50% of the selected ions in each subpopulation have unfolded at an activation voltage of 22 V (Figure 3A, Table S2 in the Supporting Information). However, the peak centers and peak widths of the initially selected compact subpopulations are maintained (Figure 3B,C). Hence, within the limits set by the TIMS-2 resolving power, the spectra reveal no evidence for isomerization among the initially selected, compact subpopulations. (A peak shoulder is present upon activation by 24 V, but here, the survival yield is already ~10%.)

Taken together, these observations show that the unfolding and isomerization of the subpopulations are distinct, non-consecutive reactions, and, further, that the free energy barriers

https://doi.org/10.1021/jacs.3c12892
J. Am. Chem. Soc. XXXX, XXX, XXX−XXX

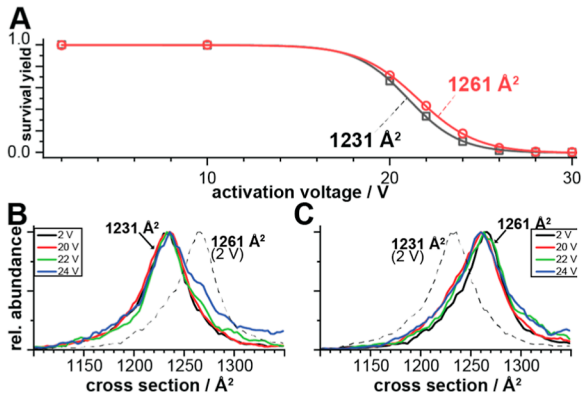

Figure 3. (A) Survival yields of ubiquitin charge state 7+ subpopulations with cross sections of 1231 and 1261 Å^2 upon activation by up to 35 V. Survival yield is ~50% upon activation by 22 V (traces: hill survival function fit to the data). (B,C) Peak centers and widths of the subpopulations are maintained upon energetic activation up to ~22 V. Hence, energetic activation of the subpopulations centered at ~1230 and ~1260 Å^2 does not induce their isomerization. All cross sections were recorded in nitrogen gas. Survival yields are calculated as the overlap between the spectrum at a given activation voltage and that of the nonactivated spectrum.

for unfolding are lower than those for isomerization. Hence, the most likely scenario is that the ubiquitin subpopulations observed in the absence of a solvent originate from structurally distinct solution-phase precursors. This view is consistent with prior literature indicating that an ensemble of protein solution conformations leads to an ensemble of solvent-free protein conformations.[21,27,77,79,81−83]

Unfolding of Compact, Solvent-Free Proteins Exhibits Stretched-Exponential Time Dependence. Our discussion above indicates that the motions of the initially selected, compact subpopulations are confined into disjoint regions in configuration space. This points to a rugged energy landscape in the solvent-free environment, which prompted us to investigate the structural relaxation kinetics of the solvent-free ubiquitin (sub)populations.

To this end, we mobility-selected ubiquitin ions eluting from TIMS-1 and stored the selected ions in TIMS-2 for up to ~21 s before recording ion mobility spectra. Figure 4 shows the resulting time-resolved ion mobility spectra for the compact feature of charge states 6+ and 7+. The corresponding time-resolved spectra for the compact populations of charge state 8+ for ubiquitin are given in Figure S6 (Supporting Information). As controls, we recorded time-resolved spectra for lysozyme (charge state 8+), the partially unfolded feature of charge state 7+ of ubiquitin (aqueous solution, after collisional activation), and the partially unfolded feature of charge state 8+ of ubiquitin from acidic methanol/water (see Figures S5−S8, Supporting Information, for details).

The time-resolved spectra show the structural relaxation of compact ubiquitin (charge states 6+ to 8+) into a stable, unfolded species (1800−2000 Å^2) proceeds *via* a partially unfolded intermediate (1400−1700 Å^2). The unfolded and partially unfolded species are consistent with those observed by CIU (Figure S4 in the Supporting Information). However, a difference to the CIU spectra is the emergence of an elongated

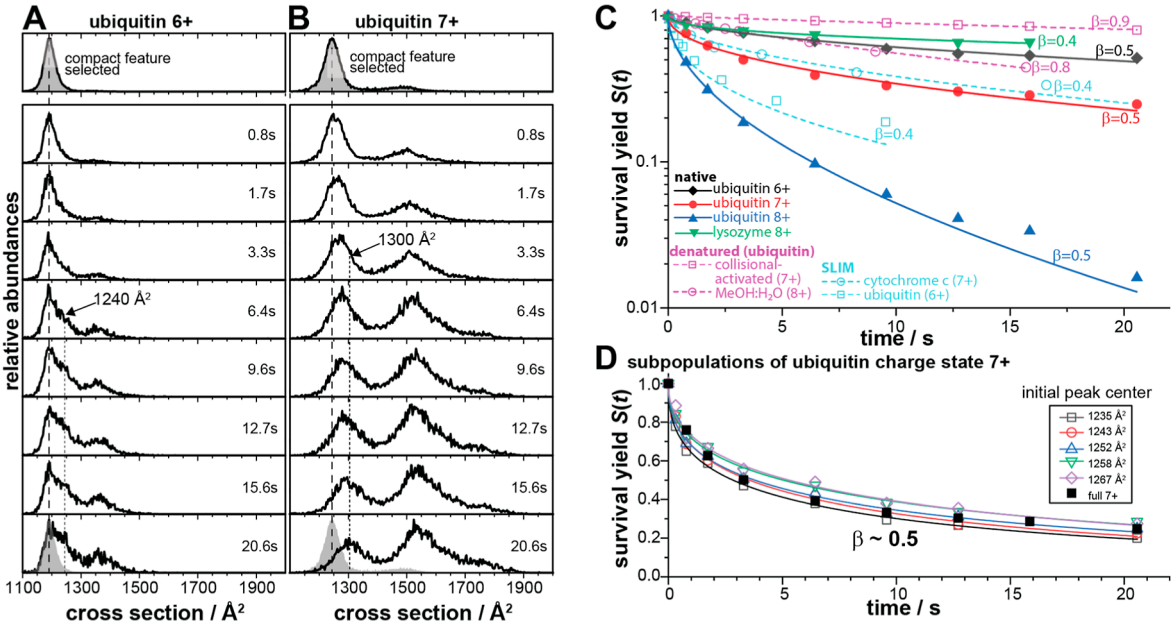

Figure 4. Unfolding of compact proteins shows stretched-exponential time dependence with a stretching coefficient β of ~0.5. (A,B) Time-resolved ion mobility spectra for ubiquitin charge states 6+ and 7+. The compact feature was selected and stored in the absence of a solvent for up to ~21 s, showing the formation of a transiently populated intermediate at cross sections of ~1250 Å^2 (6+) and ~1300 Å^2 (7+), respectively, before a partially unfolded species at ~1400 Å^2 (6+) and ~1550 Å^2 (7+), respectively, emerges. (C) Survival yields $S(t)$ for native-like ubiquitin (6+, 7+, and 8+) and lysozyme 8+ (filled symbols), non-native (partially unfolded) ubiquitin (7+, 8+, pink, open symbols) calculated as the overlap between the compact feature of the mobility-selected spectrum and the spectrum after storage. SLIM measurements (cyan, open symbols) were taken from ref 31 (ubiquitin 6+) and 27 (cytochrome *c* 7+). The traces show fitted stretched exponentials $S(t) = \exp[-(kt)^{\beta}]$ underlining stretched-exponential time dependence for the folded, compact species ($\beta \approx 0.4$−0.5) but single-exponential kinetics for the denatured (partially unfolded) species ($\beta \approx 0.8$ and 0.9). (D) Survival yields $S(t)$ of compact ubiquitin subpopulations of charge state 7+ revealing a stretched-exponential time dependence of $\beta \sim 0.5$ for all subpopulations. Cross sections were measured in nitrogen.

https://doi.org/10.1021/jacs.3c12892
J. Am. Chem. Soc. XXXX, XXX, XXX−XXX

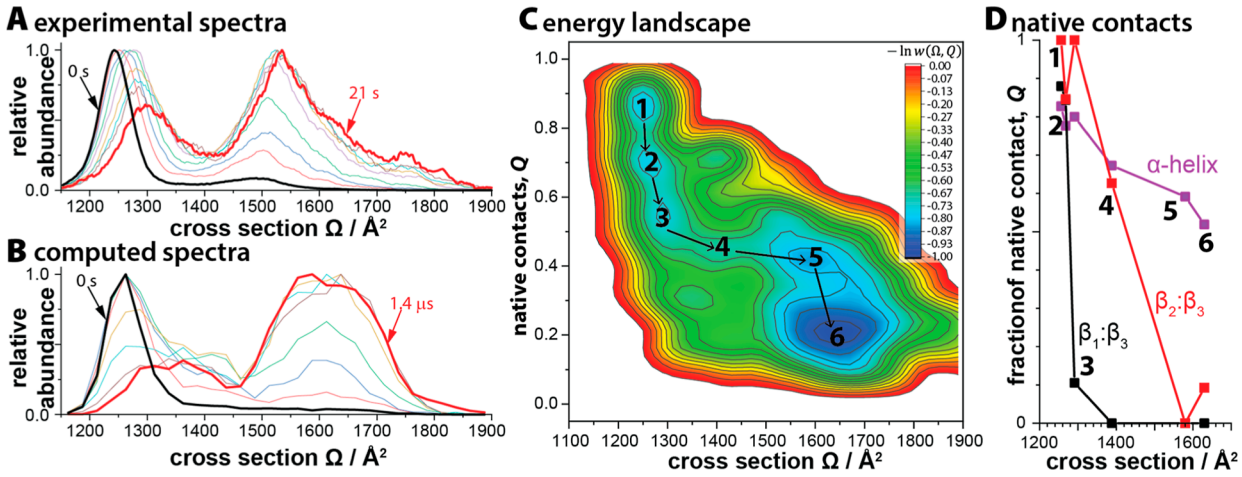

Figure 5. Solvent-free ubiquitin unfolds on a rugged energy landscape *via* a highly polarized transition state with native character on the N-terminus. (A,B) Experimental and computed time-dependent ion mobility spectra for ubiquitin charge state 7+ (Pearson correlation coefficients range from 0.7 to 0.9). The ion abundances partition into two regions of significant intensity that are separated by a minimum of around 1400 Å^2. (C) Normalized energy landscape $-\ln w(\Omega,Q)$ compiled from MD simulations, where $w(\Omega,Q)$ is the number of snaphots with cross section Ω and the fraction of native contacts Q. The computed landscape partitions into two broad basins of compact (**1**−**3**; Ω < 1400 Å^2) and partially unfolded (**5**, **6**; Ω > 1500 Å^2) conformations. These two basins are connected by a "bottleneck" **4** in the computed landscape at cross sections of roughly 1460 Å^2, closely matching the free energy maximum inferred from the experimental spectra at a cross section of ∼1400 Å^2. (D) Loss of native contacts during the unfolding process from conformation **1** to **6** in (C). Nitrogen cross sections.

yet compact transient intermediate (∼1250 Å^2 for charge state 6+ and ∼1300 Å^2 for charge states 7+ and 8+), discussed in the next section. For kinetic analysis, we show the survival yields $S(t)$ in Figure 4C along with prior data for cytochrome *c* and ubiquitin recorded on structures for lossless ion manipulation (SLIM)-type instruments.[27,31]

A two-state reaction results in single-exponential kinetics according to $S(t) = \exp(-kt)$. Such exponential kinetics are observed for the structural relaxation of the denatured (partially unfolded) ubiquitin species, but excluded for all compact protein species from nondenaturing conditions (Figures 4 and S7 and S9, Supporting Information). We further discarded all kinetic models that posit an equilibrium between the compact and the partially unfolded species because structural relaxation of the partially unfolded species did not produce detectable amounts of compact ubiquitin conformations (Figure S7, Supporting Information). A double-exponential rate law explains $S(t)$ with high confidence, in line with literature reports,[25−27] but this leads to overfitting even for its 3-parameter form (Figure S10, Supporting Information) and renders the physical meaning of the fit questionable.

By contrast, high goodness of fit was achieved without overfitting for the simpler stretched-exponential rate law $S(t) = \exp[-(kt)^{\beta}]$ with only the rate constant k and the stretching coefficient β as fitting parameters (Figure 4 and Tables S3 and S4, Supporting Information). The resulting rate constants k increase roughly 25-fold from charge states 6+ to 8+ of ubiquitin, as expected from literature reports.[21,25,31] What is more intriguing is that the corresponding stretching coefficients β for the compact, native-like protein systems cluster around $\beta \approx$ 0.4 to 0.5, indicative of a strongly stretched-exponential relaxation process.[84] By contrast, the stretching coefficients for the denatured controls are $\beta \approx 0.8$ and $\beta \approx 0.9$, respectively, more in line with a single-exponential, two-state reaction. Thus, time-resolved measurements for three proteins on two distinct IM/MS types suggest that the structural relaxation of compact, native-like proteins is strongly stretched-exponential.

A structural relaxation process with stretched-exponential kinetics can have two different origins.[85] One scenario is that of a rough free energy landscape with kinetic traps; the alternative scenario is that of an ensemble of unresolved species that each relax exponentially but with a broad distribution of rate constants. To distinguish between these scenarios, we characterized the relaxation process of mobility-selected ubiquitin subpopulations with cross sections ranging from 1235 to 1267 Å^2 (see Figure 4D and the Supporting Information for Tables S4, S6 and Figure S12). We make two main observations from the time-resolved spectra of the mobility-selected subpopulations. First, all selected subpopulations transiently populate an intermediate with a cross section of ∼1300 Å^2 before the partially unfolded species is formed centered at ∼1525 Å^2. Further, the positions and relative abundances of the transient intermediate at ∼1300 Å^2 and partially unfolded species centered at ∼1525 Å^2 appear to be comparable for all subpopulations at all trapping times. These observations indicate that the unfolding pathways are similar for the subpopulations. Second, fitting the survival yields $S(t)$ to stretched exponentials results in stretching coefficients $\beta \approx 0.5$ for all subpopulations, in line with the value obtained for the entire compact population of charge state 7+ (Figure 4C and Table S4, Supporting Information).

In sum, the unfolding of three compact protein systems, including their subpopulations, recorded on two distinct ion mobility/mass spectrometers showed stretched-exponential time dependence ($\beta \sim 0.4$−0.5). By contrast, denatured species show single-exponential time dependence ($\beta \sim 0.8$−0.9). Because the stretched exponential function is economical with only two fitting parameters, it seems unlikely that the success of fitting all of the data shown here in a consistent manner is entirely by accident. Hence, our data are most consistent with the view that a rugged free energy landscape leads to the stretched-exponential unfolding of ubiquitin in the absence of a solvent.

Stretched-Exponential Time-Dependent Relaxation Arises from a Rugged Energy Landscape. To interpret

https://doi.org/10.1021/jacs.3c12892
J. Am. Chem. Soc. XXXX, XXX, XXX−XXX

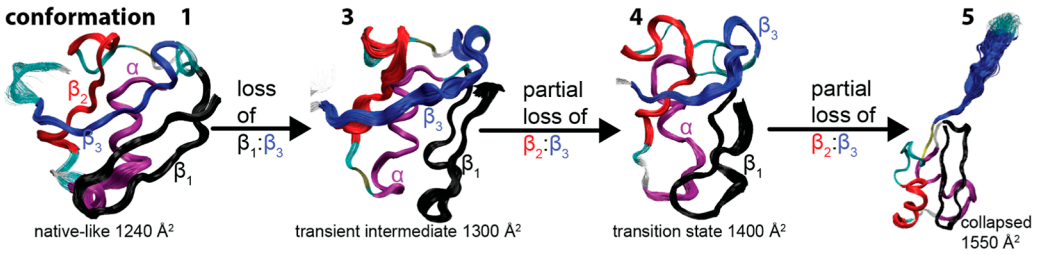

Figure 6. Proposed unfolding mechanism of solvent-free ubiquitin. Loss of native contacts predominates in the first step **1** → **3** and leads to separation of β-strands β_1 and β_3. Subsequently, β_2 and β_3 separate from each other (**3** → **5**) *via* polarized transition state **4** that maintains native contacts at the N-terminal region. This results in a partially unfolded, collapsed state **5** with native content in the N-terminal region. Shown are averaged structures representative of the species indicated in Figure 5C.

the structural changes occurring in the time-resolved unfolding measurements, we simulated the unfolding of compact ubiquitin charge state 7+. To this end, we propagated each of the >1000 structures computed by the SRA for the compact feature of charge state 7+ (Figure 2D) for 3 μs at 450 K using solvent-free MD simulations and calculated cross sections using our PSA method for structures sampled every 2 ns. We then used the "reactive" trajectories that reached the partially unfolded species with cross sections >1500 Å^2 to compute time-dependent ion mobility spectra (Section S6, Supporting Information).

We observe a strong consistency between the experimental and computed time-resolved ion mobility spectra (Figure 5A,B; Pearson correlation coefficients ranging from 0.7 to 0.9). Notably, the computed spectra reproduce the main features of the time-dependent experimental spectra: (1) a decrease of the abundances of the initially selected compact feature; (2) transient formation of an intermediate species with a cross section of ~1300 Å^2; (3) a minimum of the ion abundances for cross sections between ~1400 and 1450 Å^2; (4) the emergence of a pronounced broad feature from 1450 to 1800 Å^2 corresponding to the partially folded species; (5) stretched-exponential unfolding kinetics (Figure S18, Supporting Information; stretching coefficient $\beta \sim 0.67$). The main difference is the much shorter time scale of the simulations; this is due to the necessity of choosing a simulation temperature that significantly exceeds the experimental ion temperature because current MD techniques do not allow the simulation of reactions occurring on the ~20 s time scale (Section S6, Supporting Information). Nevertheless, the computed spectra reproduce all pertinent features of the experimental spectra.

Given this agreement, one can use the simulations to determine the motions of the structural transitions in the experimental spectra. To this end, we approximated an energy landscape from the simulations as $-\ln w(\Omega,Q)$, where $w(\Omega,Q)$ is the number of snapshots with cross section Ω and fraction of native contacts Q (Figure 5C and Section S6, Supporting Information). We then extracted the structures associated with species **1** to **6** indicated in Figure 5C and analyzed their native contacts for the different secondary structure regions of ubiquitin (Figure 5D, secondary structure elements are defined in Figure S3, Supporting Information). For the sake of clarity, we illustrate the main steps of the proposed unfolding pathway in Figure 6.

Taken together, our data suggest the following pathway for the unfolding of ubiquitin in the absence of a solvent (Figures 5D and 6). First, the C-terminal β-strand separates from the N-terminal β-hairpin, while the N-terminal β-hairpin and α-helix remain strongly native. This occurs *via* several steps and leads to intermediate species **3** with a cross section of ~1300 Å^2. This species maintains an overall compact structure ($\Delta\Omega \leq 5\%$) at a significant loss of native contacts ($\Delta Q \approx 0.5$). Hence, the intermediate species that emerges in the experimental data after several seconds at ~1300 Å^2 (Figures 4B, 5A, and S12, Supporting Information) is most likely non-native. Next, the C-terminal β_3-strand separates from the β_2-strand, whereas the N-terminal β-hairpin and α-helix remain strongly native. This leads across a broad energy barrier **4** associated with a substantial increase in cross section and connects to the basin of partially unfolded conformations **5** with cross sections of ~1550 Å^2. This energy barrier explains the minor experimental abundances around ~1400 Å^2 and the intensity of partially unfolded conformations with cross sections between 1450 and 1800 Å^2. Subsequently, native contacts are lost in the N-terminal β-hairpin while maintaining an overall collapsed state with a partially native α-helix in proximity to the N-terminal β-hairpin. Finally, this collapsed state can unfold to conformations with strongly elongated ubiquitin polypeptide chains (Figures S4 and S7, Supporting Information; note that this occurs on a time scale beyond the 21 s available for our measurements of charge states 6+ and 7+).

Several observations deserve comment. First, the consistent interpretation of our computational and experimental data is that the initially produced, compact ubiquitin species exists essentially as a native fold with the β-grasp motif and α-helix intact. Second, the denaturation (loss of native contacts Q, **1** → **3**) and unfolding of the polypeptide chain (**3** → **5**) are projected to be separate, consecutive events. Hence, preventing protein unfolding in IM/MS measurements may not per se indicate native-like structures. Third, because Q correlates with the enthalpic stabilization of the polypeptide chain and the cross section Ω (compactness) is a measure for its configurational entropy,[86] our data suggest the initial denaturation **1** → **3** is impeded by an increase in enthalpy, whereas the unfolding **3** → **5** is driven mainly by a gain in entropy (Table S8, Supporting Information). Hence, increasing the activation enthalpy for denaturation **1** → **3**, such as by sequestering surface-exposed side-chains by bulky ligands[34] or salts,[33] appears to stabilize solvent-free proteins close to their native structures. Fourth, the proposed "inside-out" structure[87] is not observed: in line with other proteins,[88] the ubiquitin surface is already strongly hydrophobic in solution (~50%), which our data suggest increases to ~70% for the solvent-free species **6** (Table S9, Supporting Information). Finally, our observations parallel results from variable-temperature IM/MS that showed native (solution) CI2 conformations were enthalpically stabilized, whereas denatured (solution) conformations are favored entropically.[79]

https://doi.org/10.1021/jacs.3c12892
J. Am. Chem. Soc. XXXX, XXX, XXX−XXX

Ubiquitin Unfolds through a Polarized Transition State, Regardless of the Solvent. Our analysis indicates that ubiquitin unfolding in the solvent-free environment shares many characteristics with those established for the presence of solvent:[45−47,52,53] (1) unfolding of ubiquitin starts by the separation of the C-terminal β-strand from the scaffold of ubiquitin, and this step occurs on the folded side of the transition state. (2) The transition state appears polarized with a predominant native structure in the N-terminal region of the β-hairpin and the α-helix. In contrast, the remainder of the polypeptide chain does not exhibit a strongly native character. (3) At the unfolded side of the transition state, a collapsed state maintains a nucleus by closely packing the N-terminal β-hairpin and α-helix, both with some extent of native character. (4) Mirroring our observation of a transient intermediate **3** with significantly reduced native β-content (Figures 5 and 6), 2D IR spectroscopy detected an on-pathway folding intermediate located between the folded state and the unfolding transition state, showing disrupted β-content.[89] (5) The folded state seems favored by enthalpic stabilization due to native contacts, whereas the unfolded state appears favored by entropy.[51] Nevertheless, a major difference appears to be the unfolding rate, which is approximately 800 to 20,000 times faster in the presence of water ($k_u^{H_2O} \sim 620\ s^{-1}$ *vs* $k_u \sim 0.03$ to $\sim 0.8\ s^{-1}$ for charge states 6+ to 8+, see Table S3, Supporting Information),[47] effectively quenching the unfolding in the absence of a solvent.

Our data thus indicate that the unfolding of ubiquitin, a large-scale motion that significantly alters the protein shape, is similar in the presence and absence of a solvent, albeit much slower. Hence, our data here suggest (1) that the solvent determines the free energy differences between the folded and unfolded states and activates their isomerization rates; and (2) that structural events in the folding of ubiquitin are at least partially encoded by its amino acid sequence.

These considerations appear intriguing considering the established view that slow protein motions involving shape changes are driven by the so-called α-relaxation of the solvent: such protein motions exhibit the same non-Arrhenius temperature-dependence and nonexponential time-dependence as the rate of the solvent fluctuations, depend noticeably on solvent viscosity, and are absent when the protein is embedded in a solid or dehydrated.[16,17,90−92] We explain this apparent deviation from the established view by the fact that prior work measured the protein dynamics of dehydrated proteins in bulk, *i.e.*, within a solid surrounding that sterically hampers protein motions that induce large-scale shape changes. By contrast, our experiments characterize the protein dynamics of individual, solvent-free proteins embedded in a dilute gas where no such hampering occurs. Our analysis supports the view[93] that solvent facilitates, rather than controls, protein motions.

Glassy Behavior of Solvent-Free Proteins. Finally, we draw some analogies between solvent-free proteins and glass. First, the properties of glass depend on history, that is, on the details of how the glass was formed. This also applies to solvent-free proteins in IM/MS: the observed collision cross sections and charge states depend on the history of how the solvent-free protein was generated in the IM/MS experiment.[21,22,25,80] Second, a glass is in a nonequilibrium state and relaxes toward the state of thermodynamic equilibrium on a time scale that is longer than the observation time. This also applies to solvent-free proteins in IM/MS: a folded, solvent-free protein is quenched into a nonequilibrium state and spontaneously relaxes toward a thermodynamically (more) stable state, as demonstrated by time-dependent IM/MS measurements shown here and elsewhere.[25−27,31] For "soft" IM/MS measurements, the relaxation process is too slow to be observed on typical measurement time scales.[21,29−31] Third, near and above the glass temperature, the fluctuations of a glass are dominated by the α-relaxation and exhibit non-Arrhenius temperature dependence and nonexponential time dependence.[94] The underlying cause of this behavior is a rugged energy landscape, with a plethora of conformational states and energy barriers separating them. This leads to metastable, long-lived intermediates when the thermal energy is insufficient to allow for effective sampling of the entire configuration space. The result is a stretched-exponential time-dependence with a stretching coefficient β around ~0.3 to ~0.6 for molecular and polymeric glasses.[84] As shown in our discussion above, these considerations also apply to folded, solvent-free proteins: their structural relaxation occurs on a rugged energy landscape and involves metastable intermediates, producing stretched-exponential time-dependent relaxation with stretching coefficients β of ~0.5.

These considerations suggest that the energy landscape governing the motions of folded, solvent-free proteins resembles a glassy system. Hence, it appears beneficial to apply the concepts developed for glassy systems to describe the dynamics of solvent-free protein systems.

CONCLUSIONS

We characterized ubiquitin unfolding in the absence of a solvent by a combination of computational and experimental ion mobility/ion mobility/mass spectrometry methods. To this end, we experimentally partitioned solvent-free, folded ubiquitin ions into subpopulations (Figure 2) and probed their CIU (Figure 3) and time-resolved structural relaxation processes (Figure 4). We computed ion mobility spectra for comparison to the experiments and proposed the structural changes governing the unfolding of solvent-free ubiquitin (Figures 5 and 6). Our analysis, summarized in Figure 7, suggests:

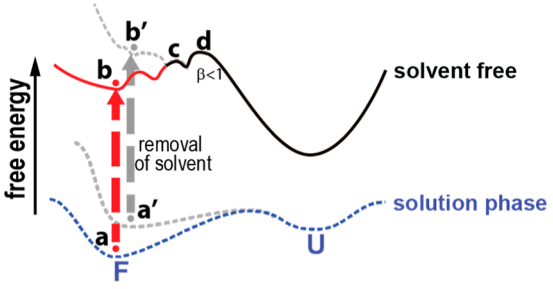

Figure 7. Energy landscapes summarize our analysis of the unfolding of solvent-free ubiquitin. Different solution conformers (a, a') populate different solvent-free subpopulations (b, b', Figures 2 and 3). The solvent-free subpopulations undergo stretched-exponential structural relaxation on a rugged energy surface, becoming non-native (c, Figures 4 and 5). The unfolding transition state (d, Figures 5 and 6) appears highly polarized with native content at the N-terminus, as proposed for the presence of solvent.

(1) Folded, solvent-free ubiquitin observed by IM/MS exists in a largely native structure with an intact β-grasp motif and α-helix.

(2) The folded, solvent-free ubiquitin subpopulations observed by IM/IM/MS reflect the structural heterogeneity of ubiquitin in solution.

https://doi.org/10.1021/jacs.3c12892
J. Am. Chem. Soc. XXXX, XXX, XXX−XXX

(3) The structural relaxation of folded, solvent-free ubiquitin exhibits a strongly stretched-exponential time dependence caused by a rugged free energy landscape with kinetic traps. The energy landscape governing the motions of folded, solvent-free ubiquitin resembles the energy landscape of a glassy system.

(4) The denaturation (loss of native contacts) and unfolding of the solvent-free ubiquitin polypeptide chain appear to be separate, consecutive events.

(5) The proposed unfolding pathway of solvent-free ubiquitin shares substantial characteristics with that established for the presence of solvent, including a polarized transition state with significant native content in the N-terminal β-hairpin and α-helix. Regardless of solvent, the folded state appears favored by enthalpic stabilization due to native contacts, whereas the unfolded state appears entropically favored. Unfolding rate constants appear to be roughly 800 to 20,000 times faster in the presence of water than in the absence of a solvent.

Taken together, our analysis supports the notions that (1) large-scale protein motions may at least partially be determined by the amino acid sequence of a polypeptide chain; and (2) solvent facilitates, rather than controls, protein motions.

How do our findings extrapolate to other proteins? Ubiquitin is a small, globular protein with a well-defined hydrophobic core and limited structural flexibility in its native state. The data shown in Figure 4 indicate that our results on ubiquitin should extrapolate in a straightforward manner to similar proteins such as lysozyme and cytochrome *c*. However, the results presented here raise questions about proteins with more complex kinetic mechanisms[95] or proteins with solvent molecules directly involved in their structures.[96,97] The enzymatic activity of ribonuclease A, for example, depends on the transition between an open and a closed conformation and their perturbations upon substrate binding.[98] Our results on ubiquitin do not allow extrapolation on whether such transitions can be retained in a solvent-free environment. Nevertheless, we emphasize that (1) large-scale protein motions often occur on the millisecond time scale and thus have larger activation energies than the submillisecond structural transitions of native ubiquitin, and (2) we observed buried solvent molecules for the protein complex avidin in the solvent-free environment.[61] Hence, although we cannot directly extrapolate our results on ubiquitin to these more complex protein systems, our technical approaches described here can be expected to address these questions in future studies.

■ ASSOCIATED CONTENT

Supporting Information

The Supporting Information is available free of charge at https://pubs.acs.org/doi/10.1021/jacs.3c12892.

Expanded experimental and computational details and time-resolved and energy-resolved IM/MS of proteins (PDF)

■ AUTHOR INFORMATION

Corresponding Author

Christian Bleiholder − *Department of Chemistry and Biochemistry, Florida State University, Tallahassee, Florida 32304, United States; Institute of Molecular Biophysics, Florida State University, Tallahassee, Florida 32304, United States;* orcid.org/0000-0002-4211-1388; Email: cbleiholder@fsu.edu

Authors

Tyler. C. Cropley − *Department of Chemistry and Biochemistry, Florida State University, Tallahassee, Florida 32304, United States;* orcid.org/0000-0003-2804-2555

Fanny. C. Liu − *Department of Chemistry and Biochemistry, Florida State University, Tallahassee, Florida 32304, United States;* orcid.org/0000-0003-1403-7114

Mengqi Chai − *Department of Chemistry and Biochemistry, Florida State University, Tallahassee, Florida 32304, United States;* orcid.org/0000-0002-6363-0216

Matthew F. Bush − *Department of Chemistry, University of Washington, Seattle, Washington 98195-1700, United States;* orcid.org/0000-0003-3526-4973

Complete contact information is available at: https://pubs.acs.org/10.1021/jacs.3c12892

Author Contributions

T.C.C. and F.C.L. authors contributed equally. All authors have given approval to the final version of the manuscript.

Notes

The authors declare no competing financial interest.

■ ACKNOWLEDGMENTS

The authors thank Dr. Thais Pedrete for assistance in carrying out some of the time-dependent measurements. This work was supported by the National Institutes of Health under grant R01GM135682 (C.B.) and by the National Science Foundation under grants no. CHE-1654608 (C.B.) and CHE-2305173 (C.B. and F.C.L.). The research reported in this publication was supported by the National Institute of General Medical Sciences of the National Institutes of Health through award number R01GM130708 (M.F.B.).

■ REFERENCES

(1) Perutz, M. F.; Brunori, M. Stereochemistry of Cooperative Effects in Fish and Amphibian Haemoglobins. *Nature* **1982**, *299* (5882), 421−426.

(2) Onuchic, J. N.; Wolynes, P. G. Theory of Protein Folding. *Curr. Opin. Struct. Biol.* **2004**, *14* (1), 70−75.

(3) Frauenfelder, H.; Sligar, S. G.; Wolynes, P. G. The Energy Landscapes and Motions of Proteins. *Science* **1991**, *254* (5038), 1598−1603.

(4) Dobson, C. M.; Šali, A.; Karplus, M. Protein Folding: A Perspective from Theory and Experiment. *Angew. Chem., Int. Ed.* **1998**, *37* (7), 868−893.

(5) Li, Y. I.; van de Geijn, B.; Raj, A.; Knowles, D. A.; Petti, A. A.; Golan, D.; Gilad, Y.; Pritchard, J. K. RNA Splicing Is a Primary Link between Genetic Variation and Disease. *Science* **2016**, *352* (6285), 600−604.

(6) Benesch, J. L. P.; Ruotolo, B. T.; Simmons, D. A.; Robinson, C. V. Protein Complexes in the Gas Phase: Technology for Structural Genomics and Proteomics. *Chem. Rev.* **2007**, *107* (8), 3544−3567.

(7) Laganowsky, A.; Reading, E.; Allison, T. M.; Ulmschneider, M. B.; Degiacomi, M. T.; Baldwin, A. J.; Robinson, C. V. Membrane Proteins Bind Lipids Selectively to Modulate Their Structure and Function. *Nature* **2014**, *510* (7503), 172−175.

(8) Roberts, D. S.; Mann, M.; Melby, J. A.; Larson, E. J.; Zhu, Y.; Brasier, A. R.; Jin, S.; Ge, Y. Structural O-Glycoform Heterogeneity of the SARS-CoV-2 Spike Protein Receptor-Binding Domain Revealed by Top-Down Mass Spectrometry. *J. Am. Chem. Soc.* **2021**, *143* (31), 12014−12024.

(9) Bernstein, S. L.; Dupuis, N. F.; Lazo, N. D.; Wyttenbach, T.; Condron, M. M.; Bitan, G.; Teplow, D. B.; Shea, J.-E.; Ruotolo, B. T.; Robinson, C. V.; Bowers, M. T. Amyloid-β protein oligomerization and the importance of tetramers and dodecamers in the aetiology of Alzheimer's disease. *Nat. Chem.* **2009**, *1* (4), 326−331.
(10) Bleiholder, C.; Dupuis, N. F.; Wyttenbach, T.; Bowers, M. T. Ion mobility−mass spectrometry reveals a conformational conversion from random assembly to β-sheet in amyloid fibril formation. *Nat. Chem.* **2011**, *3* (2), 172−177.
(11) Callaway, D. J. E. Solvent-Induced Organization: A Physical Model of Folding Myoglobin. *Proteins Struct. Funct. Genet.* **1994**, *20* (2), 124−138.
(12) Ruotolo, B. T.; Hyung, S.-J.; Robinson, P. M.; Giles, K.; Bateman, R. H.; Robinson, C. V. Ion Mobility-Mass Spectrometry Reveals Long-Lived, Unfolded Intermediates in the Dissociation of Protein Complexes. *Angew. Chem., Int. Ed.* **2007**, *46*, 8001−8004.
(13) Nash, S.; Vachet, R. W. Gas-Phase Unfolding of Protein Complexes Distinguishes Conformational Isomers. *J. Am. Chem. Soc.* **2022**, *144* (48), 22128−22139.
(14) Allen, S. J.; Giles, K.; Gilbert, T.; Bush, M. F. Ion Mobility Mass Spectrometry of Peptide, Protein, and Protein Complex Ions Using a Radio-Frequency Confining Drift Cell. *Analyst* **2016**, *141* (3), 884−891.
(15) Beveridge, R.; Migas, L. G.; Das, R. K.; Pappu, R. V.; Kriwacki, R. W.; Barran, P. E. Ion Mobility Mass Spectrometry Uncovers the Impact of the Patterning of Oppositely Charged Residues on the Conformational Distributions of Intrinsically Disordered Proteins. *J. Am. Chem. Soc.* **2019**, *141* (12), 4908−4918.
(16) Fenimore, P. W.; Frauenfelder, H.; McMahon, B. H.; Parak, F. G. Slaving: Solvent Fluctuations Dominate Protein Dynamics and Functions. *Proc. Natl. Acad. Sci. U.S.A.* **2002**, *99* (25), 16047−16051.
(17) Frauenfelder, H.; Chen, G.; Berendzen, J.; Fenimore, P. W.; Jansson, H.; McMahon, B. H.; Stroe, I. R.; Swenson, J.; Young, R. D. A Unified Model of Protein Dynamics. *Proc. Natl. Acad. Sci. U.S.A.* **2009**, *106* (13), 5129−5134.
(18) Breuker, K.; McLafferty, F. W. Stepwise Evolution of Protein Native Structure with Electrospray into the Gas Phase, 10−12 to 102 s. *Proc. Natl. Acad. Sci. U.S.A.* **2008**, *105* (47), 18145−18152.
(19) Barron, L. D.; Hecht, L.; Wilson, G. The Lubricant of Life: A Proposal That Solvent Water Promotes Extremely Fast Conformational Fluctuations in Mobile Heteropolypeptide Structure. *Biochemistry* **1997**, *36* (43), 13143−13147.
(20) Lee, S.-W.; Freivogel, P.; Schindler, T.; Beauchamp, J. L. Freeze-Dried Biomolecules: FT-ICR Studies of the Specific Solvation of Functional Groups and Clathrate Formation Observed by the Slow Evaporation of Water from Hydrated Peptides and Model Compounds in the Gas Phase. *J. Am. Chem. Soc.* **1998**, *120* (45), 11758−11765.
(21) Wyttenbach, T.; Bowers, M. T. Structural Stability from Solution to the Gas Phase: Native Solution Structure of Ubiquitin Survives Analysis in a Solvent-Free Ion Mobility-Mass Spectrometry Environment. *J. Phys. Chem. B* **2011**, *115* (42), 12266−12275.
(22) Koeniger, S. L.; Merenbloom, S. I.; Sevugarajan, S.; Clemmer, D. E. Transfer of Structural Elements from Compact to Extended States in Unsolvated Ubiquitin. *J. Am. Chem. Soc.* **2006**, *128* (35), 11713−11719.
(23) Breuker, K.; Oh, H.; Horn, D. M.; Cerda, B. A.; McLafferty, F. W. Detailed Unfolding and Folding of Gaseous Ubiquitin Ions Characterized by Electron Capture Dissociation. *J. Am. Chem. Soc.* **2002**, *124* (22), 6407−6420.
(24) Jurneczko, E.; Barran, P. E. How Useful Is Ion Mobility Mass Spectrometry for Structural Biology? The Relationship between Protein Crystal Structures and Their Collision Cross Sections in the Gas Phase. *Analyst* **2011**, *136* (1), 20−28.
(25) Myung, S.; Badman, E. R.; Lee, Y. J.; Clemmer, D. E. Structural Transitions of Electrosprayed Ubiquitin Ions Stored in an Ion Trap over ~ 10 Ms to 30 s. *J. Phys. Chem. A* **2002**, *106* (42), 9976−9982.
(26) Badman, E. R.; Hoaglund-Hyzer, C. S.; Clemmer, D. E. Monitoring Structural Changes of Proteins in an Ion Trap over ~ 10−200 Ms: Unfolding Transitions in Cytochrome c Ions. *Anal. Chem.* **2001**, *73* (24), 6000−6007.
(27) Allen, S. J.; Eaton, R. M.; Bush, M. F. Structural Dynamics of Native-Like Ions in the Gas Phase: Results from Tandem Ion Mobility of Cytochrome c. *Anal. Chem.* **2017**, *89* (14), 7527−7534.
(28) Ruotolo, B. T.; Giles, K.; Campuzano, I.; Sandercock, A. M.; Bateman, R. H.; Robinson, C. V. Evidence for Macromolecular Protein Rings in the Absence of Bulk Water. *Science* **2005**, *310* (5754), 1658−1661.
(29) Bleiholder, C.; Liu, F. C. Structure Relaxation Approximation (SRA) for Elucidation of Protein Structures from Ion Mobility Measurements. *J. Phys. Chem. B* **2019**, *123* (13), 2756−2769.
(30) Laszlo, K. J.; Munger, E. B.; Bush, M. F. Folding of Protein Ions in the Gas Phase after Cation-to-Anion Proton-Transfer Reactions. *J. Am. Chem. Soc.* **2016**, *138* (30), 9581−9588.
(31) Zercher, B. P.; Hong, S.; Roush, A. E.; Feng, Y.; Bush, M. F. Are the Gas-Phase Structures of Molecular Elephants Enduring or Ephemeral? Results from Time-Dependent, Tandem Ion Mobility. *Anal. Chem.* **2023**, *95* (25), 9589−9597.
(32) Steinberg, M. Z.; Breuker, K.; Elber, R.; Gerber, R. B. The Dynamics of Water Evaporation from Partially Solvated Cytochrome c in the Gas Phase. *Phys. Chem. Chem. Phys.* **2007**, *9* (33), 4690.
(33) Wagner, N. D.; Kim, D.; Russell, D. H. Increasing Ubiquitin Ion Resistance to Unfolding in the Gas Phase Using Chloride Adduction: Preserving More "Native-Like" Conformations Despite Collisional Activation. *Anal. Chem.* **2016**, *88* (11), 5934−5940.
(34) Warnke, S.; Von Helden, G.; Pagel, K. Protein Structure in the Gas Phase: The Influence of Side-Chain Microsolvation. *J. Am. Chem. Soc.* **2013**, *135* (4), 1177−1180.
(35) Zhou, L.; Liu, Z.; Guo, Y.; Liu, S.; Zhao, H.; Zhao, S.; Xiao, C.; Feng, S.; Yang, X.; Wang, F. Ultraviolet Photodissociation Reveals the Molecular Mechanism of Crown Ether Microsolvation Effect on the Gas-Phase Native-like Protein Structure. *J. Am. Chem. Soc.* **2023**, *145* (2), 1285−1291.
(36) Abramsson, M. L.; Sahin, C.; Hopper, J. T. S.; Branca, R. M. M.; Danielsson, J.; Xu, M.; Chandler, S. A.; Österlund, N.; Ilag, L. L.; Leppert, A.; Costeira-Paulo, J.; Lang, L.; Teilum, K.; Laganowsky, A.; Benesch, J. L. P.; Oliveberg, M.; Robinson, C. V.; Marklund, E. G.; Allison, T. M.; Winther, J. R.; Landreh, M. Charge Engineering Reveals the Roles of Ionizable Side Chains in Electrospray Ionization Mass Spectrometry. *JACS Au* **2021**, *1* (12), 2385−2393.
(37) Bryngelson, J. D.; Onuchic, J. N.; Socci, N. D.; Wolynes, P. G. Funnels, Pathways, and the Energy Landscape of Protein Folding: A Synthesis. *Proteins Struct. Funct. Genet.* **1995**, *21* (3), 167−195.
(38) Matouschek, A.; Kellis, J. T.; Serrano, L.; Fersht, A. R. Mapping the Transition State and Pathway of Protein Folding by Protein Engineering. *Nature* **1989**, *340* (6229), 122−126.
(39) Jackson, S. E.; elMasry, N.; Fersht, A. R. Structure of the Hydrophobic Core in the Transition State for Folding of Chymotrypsin Inhibitor 2: A Critical Test of the Protein Engineering Method of Analysis. *Biochemistry* **1993**, *32* (42), 11270−11278.
(40) Fersht, A. R.; Sato, S. -Value Analysis and the Nature of Protein-Folding Transition States. *Proc. Natl. Acad. Sci. U.S.A.* **2004**, *101* (21), 7976−7981.
(41) Sabelko, J.; Ervin, J.; Gruebele, M. Observation of Strange Kinetics in Protein Folding. *Proc. Natl. Acad. Sci. U.S.A.* **1999**, *96* (11), 6031−6036.
(42) Rasmussen, B. F.; Stock, A. M.; Ringe, D.; Petsko, G. A. Crystalline Ribonuclease A Loses Function below the Dynamical Transition at 220 K. *Nature* **1992**, *357* (6377), 423−424.
(43) Karplus, M.; Vitkup, D.; Ringe, D.; Petsko, G. A. Solvent Mobility and the Protein 'Glass' Transition. *Nat. Struct. Biol.* **2000**, *7* (1), 34−38.
(44) Liu, F. C.; Ridgeway, M. E.; Park, M. A.; Bleiholder, C. Tandem Trapped Ion Mobility Spectrometry. *Analyst* **2018**, *143* (10), 2249−2258.
(45) Went, H. M.; Benitez-Cardoza, C. G.; Jackson, S. E. Is an Intermediate State Populated on the Folding Pathway of Ubiquitin? *FEBS Lett.* **2004**, *567* (2−3), 333−338.
(46) Piana, S.; Lindorff-Larsen, K.; Shaw, D. E. Atomic-Level Description of Ubiquitin Folding. *Proc. Natl. Acad. Sci. U.S.A.* **2013**, *110* (15), 5915−5920.

https://doi.org/10.1021/jacs.3c12892
J. Am. Chem. Soc. XXXX, XXX, XXX−XXX

(47) Went, H. M.; Jackson, S. E. Ubiquitin Folds through a Highly Polarized Transition State. *Protein Eng. Des. Sel.* **2005**, *18* (5), 229−237.
(48) Vijay-Kumar, S.; Bugg, C. E.; Wilkinson, K. D.; Cook, W. J. Three-Dimensional Structure of Ubiquitin at 2.8 A Resolution. *Proc. Natl. Acad. Sci. U.S.A.* **1985**, *82* (11), 3582−3585.
(49) Lange, O. F.; Lakomek, N.-A.; Farès, C.; Schröder, G. F.; Walter, K. F. A.; Becker, S.; Meiler, J.; Grubmüller, H.; Griesinger, C.; de Groot, B. L. Recognition Dynamics Up to Microseconds Revealed from an RDC-Derived Ubiquitin Ensemble in Solution. *Science* **2008**, *320* (5882), 1471−1475.
(50) Crespo, M. D.; Simpson, E. R.; Searle, M. S. Population of On-Pathway Intermediates in the Folding of Ubiquitin. *J. Mol. Biol.* **2006**, *360* (5), 1053−1066.
(51) Jourdan, M.; Searle, M. S. Insights into the Stability of Native and Partially Folded States of Ubiquitin: Effects of Cosolvents and Denaturants on the Thermodynamics of Protein Folding. *Biochemistry* **2001**, *40* (34), 10317−10325.
(52) Vallée-Bélisle, A.; Michnick, S. W. Multiple Tryptophan Probes Reveal That Ubiquitin Folds via a Late Misfolded Intermediate. *J. Mol. Biol.* **2007**, *374* (3), 791−805.
(53) Chung, H. S.; Ganim, Z.; Jones, K. C.; Tokmakoff, A. Transient 2D IR Spectroscopy of Ubiquitin Unfolding Dynamics. *Proc. Natl. Acad. Sci. U.S.A.* **2007**, *104* (36), 14237−14242.
(54) Kony, D. B.; Hünenberger, P. H.; van Gunsteren, W. F. Molecular Dynamics Simulations of the Native and Partially Folded States of Ubiquitin: Influence of Methanol Cosolvent, pH, and Temperature on the Protein Structure and Dynamics. *Protein Sci.* **2007**, *16* (6), 1101−1118.
(55) Brutscher, B.; Brüschweiler, R.; Ernst, R. R. Backbone Dynamics and Structural Characterization of the Partially Folded A State of Ubiquitin by $^{1}H^{13}$, C, and ^{15}N Nuclear Magnetic Resonance Spectroscopy. *Biochemistry* **1997**, *36* (42), 13043−13053.
(56) Michelmann, K.; Silveira, J. A.; Ridgeway, M. E.; Park, M. A. Fundamentals of Trapped Ion Mobility Spectrometry. *J. Am. Soc. Mass Spectrom.* **2015**, *26* (1), 14−24.
(57) Fernandez-Lima, F. A.; Kaplan, D. A.; Park, M. A. Note: Integration of Trapped Ion Mobility Spectrometry with Mass Spectrometry. *Rev. Sci. Instrum.* **2011**, *82* (12), 126106.
(58) Liu, F. C.; Kirk, S. R.; Bleiholder, C. On the Structural Denaturation of Biological Analytes in Trapped Ion Mobility Spectrometry—Mass Spectrometry. *Analyst* **2016**, *141* (12), 3722−3730.
(59) Bleiholder, C.; Liu, F. C.; Chai, M. Comment on Effective Temperature and Structural Rearrangement in Trapped Ion Mobility Spectrometry. *Anal. Chem.* **2020**, *92* (24), 16329−16333.
(60) Chai, M.; Bleiholder, C. Structure-Elucidation of Human CCL5 by Integrating Trapped Ion Mobility Spectrometry-Mass Spectrometry (TIMS-MS) with Structure Relaxation Approximation (SRA) Analysis. *Int. J. Mass Spectrom.* **2021**, *469*, 116682.
(61) Liu, F. C.; Cropley, T. C.; Ridgeway, M. E.; Park, M. A.; Bleiholder, C. Structural Analysis of the Glycoprotein Complex Avidin by Tandem-Trapped Ion Mobility Spectrometry-Mass Spectrometry (Tandem-TIMS/MS). *Anal. Chem.* **2020**, *92* (6), 4459−4467.
(62) Cropley, T. C.; Liu, F. C.; Pedrete, T.; Hossain, M. A.; Agar, J. N.; Bleiholder, C. Structure Relaxation Approximation (SRA) for Elucidation of Protein Structures from Ion Mobility Measurements (II). Protein Complexes. *J. Phys. Chem. B* **2023**, *127* (25), 5553−5565.
(63) Kirk, S. R.; Liu, F. C.; Cropley, T. C.; Carlock, H. R.; Bleiholder, C. On the Preservation of Non-Covalent Peptide Assemblies in a Tandem-Trapped Ion Mobility Spectrometer-Mass Spectrometer (TIMS-TIMS-MS). *J. Am. Soc. Mass Spectrom.* **2019**, *30* (7), 1204−1212.
(64) Liu, F. C.; Cropley, T. C.; Bleiholder, C. Elucidating Structures of Protein Complexes by Collision-Induced Dissociation at Elevated Gas Pressures. *J. Am. Soc. Mass Spectrom.* **2023**, *34* (10), 2247−2258.
(65) Liu, F. C.; Kirk, S. R.; Caldwell, K. A.; Pedrete, T.; Meier, F.; Bleiholder, C. Tandem Trapped Ion Mobility Spectrometry/Mass Spectrometry (tTIMS/MS) Reveals Sequence-Specific Determinants of Top-Down Protein Fragment Ion Cross Sections. *Anal. Chem.* **2022**, *94* (23), 8146−8155.
(66) Hernandez, D. R.; DeBord, J. D.; Ridgeway, M. E.; Kaplan, D. A.; Park, M. A.; Fernandez-Lima, F. Ion Dynamics in a Trapped Ion Mobility Spectrometer. *Analyst* **2014**, *139* (8), 1913−1921.
(67) Chai, M.; Young, M. N.; Liu, F. C.; Bleiholder, C. A Transferable, Sample-Independent Calibration Procedure for Trapped Ion Mobility Spectrometry (TIMS). *Anal. Chem.* **2018**, *90* (15), 9040−9047.
(68) Silveira, J. A.; Ridgeway, M. E.; Park, M. A. High Resolution Trapped Ion Mobility Spectrometery of Peptides. *Anal. Chem.* **2014**, *86* (12), 5624−5627.
(69) Stow, S. M.; Causon, T. J.; Zheng, X.; Kurulugama, R. T.; Mairinger, T.; May, J. C.; Rennie, E. E.; Baker, E. S.; Smith, R. D.; McLean, J. A.; Hann, S.; Fjeldsted, J. C. An Interlaboratory Evaluation of Drift Tube Ion Mobility-Mass Spectrometry Collision Cross Section Measurements. *Anal. Chem.* **2017**, *89* (17), 9048−9055.
(70) Lee, J.; Chai, M.; Bleiholder, C. Differentiation of Isomeric, Nonseparable Carbohydrates Using Tandem-Trapped Ion Mobility Spectrometry-Mass Spectrometry. *Anal. Chem.* **2022**, *95*, 747−757.
(71) Berendsen, H. J. C.; van der Spoel, D.; van Drunen, R. GROMACS: A Message-Passing Parallel Molecular Dynamics Implementation. *Comput. Phys. Commun.* **1995**, *91* (1−3), 43−56.
(72) Kaminski, G. A.; Friesner, R. A.; Tirado-Rives, J.; Jorgensen, W. L. Evaluation and Reparametrization of the OPLS-AA Force Field for Proteins via Comparison with Accurate Quantum Chemical Calculations on Peptides. *J. Phys. Chem. B* **2001**, *105* (28), 6474−6487.
(73) Bleiholder, C.; Wyttenbach, T.; Bowers, M. T. A Novel Projection Approximation Algorithm for the Fast and Accurate Computation of Molecular Collision Cross Sections (I). Method. *Int. J. Mass Spectrom.* **2011**, *308* (1), 1−10.
(74) Bleiholder, C.; Johnson, N. R.; Contreras, S.; Wyttenbach, T.; Bowers, M. T. Molecular Structures and Ion Mobility Cross Sections: Analysis of the Effects of He and N_2 Buffer Gas. *Anal. Chem.* **2015**, *87* (14), 7196−7203.
(75) Jeanne Dit Fouque, K.; Garabedian, A.; Leng, F.; Tse-Dinh, Y.-C.; Ridgeway, M. E.; Park, M. A.; Fernandez-Lima, F. Trapped Ion Mobility Spectrometry of Native Macromolecular Assemblies. *Anal. Chem.* **2021**, *93* (5), 2933−2941.
(76) France, A. P.; Migas, L. G.; Sinclair, E.; Bellina, B.; Barran, P. E. Using Collision Cross Section Distributions to Assess the Distribution of Collision Cross Section Values. *Anal. Chem.* **2020**, *92*, 4340−4348.
(77) Koeniger, S. L.; Merenbloom, S. I.; Clemmer, D. E. Evidence for Many Resolvable Structures within Conformation Types of Electrosprayed Ubiquitin Ions. *J. Phys. Chem. B* **2006**, *110* (13), 7017−7021.
(78) Fenwick, R. B.; Esteban-Martín, S.; Richter, B.; Lee, D.; Walter, K. F. A.; Milovanovic, D.; Becker, S.; Lakomek, N. A.; Griesinger, C.; Salvatella, X. Weak Long-Range Correlated Motions in a Surface Patch of Ubiquitin Involved in Molecular Recognition. *J. Am. Chem. Soc.* **2011**, *133* (27), 10336−10339.
(79) Raab, S. A.; El-Baba, T. J.; Woodall, D. W.; Liu, W.; Liu, Y.; Baird, Z.; Hales, D. A.; Laganowsky, A.; Russell, D. H.; Clemmer, D. E. Evidence for Many Unique Solution Structures for Chymotrypsin Inhibitor 2: A Thermodynamic Perspective Derived from vT-ESI-IMS-MS Measurements. *J. Am. Chem. Soc.* **2020**, *142* (41), 17372−17383.
(80) El-Baba, T. J.; Fuller, D. R.; Woodall, D. W.; Raab, S. A.; Conant, C. R.; Dilger, J. M.; Toker, Y.; Williams, E. R.; Russell, D. H.; Clemmer, D. E. Melting Proteins Confined in Nanodroplets with 10.6 Mm Light Provides Clues about Early Steps of Denaturation. *Chem. Commun.* **2018**, *54* (26), 3270−3273.
(81) Robinson, E. W.; Leib, R. D.; Williams, E. R. The Role of Conformation on Electron Capture Dissociation of Ubiquitin. *J. Am. Soc. Mass Spectrom.* **2006**, *17* (10), 1470−1479.
(82) Pierson, N. A.; Chen, L.; Russell, D. H.; Clemmer, D. E. Cis—Trans Isomerizations of Proline Residues Are Key to Bradykinin Conformations. *J. Am. Chem. Soc.* **2013**, *135* (8), 3186−3192.
(83) Zhou, M.; Politis, A.; Davies, R. B.; Liko, I.; Wu, K.-J.; Stewart, A. G.; Stock, D.; Robinson, C. V. Ion Mobility-Mass Spectrometry of a Rotary ATPase Reveals ATP-Induced Reduction in Conformational Flexibility. *Nat. Chem.* **2014**, *6* (3), 208−215.

https://doi.org/10.1021/jacs.3c12892
J. Am. Chem. Soc. XXXX, XXX, XXX−XXX

(84) Phillips, J. C. Stretched Exponential Relaxation in Molecular and Electronic Glasses. *Rep. Prog. Phys.* **1996**, *59* (9), 1133−1207.
(85) Ediger, M. D.; Angell, C. A.; Nagel, S. R. Supercooled Liquids and Glasses. *J. Phys. Chem.* **1996**, *100*, 13200−13212.
(86) Gruebele, M. Protein Folding: The Free Energy Surface. *Curr. Opin. Struct. Biol.* **2002**, *12* (2), 161−168.
(87) Sever, A. I. M.; Konermann, L. Gas Phase Protein Folding Triggered by Proton Stripping Generates Inside-Out Structures: A Molecular Dynamics Simulation Study. *J. Phys. Chem. B* **2020**, *124* (18), 3667−3677.
(88) Eisenhaber, F.; Argos, P. Hydrophobic Regions on Protein Surfaces: Definition Based on Hydration Shell Structure and a Quick Method for Their Computation. *Protein Eng. Des. Sel.* **1996**, *9* (12), 1121−1133.
(89) Chung, H. S.; Shandiz, A.; Sosnick, T. R.; Tokmakoff, A. Probing the Folding Transition State of Ubiquitin Mutants by Temperature-Jump-Induced Downhill Unfolding. *Biochemistry* **2008**, *47* (52), 13870−13877.
(90) Frauenfelder, H.; Alberding, N. A.; Ansari, A.; Braunstein, D.; Cowen, B. R.; Hong, M. K.; Iben, I. E. T.; Johnson, J. B.; Luck, S. Proteins and Pressure. *J. Phys. Chem.* **1990**, *94* (3), 1024−1037.
(91) Iben, I. E. T.; Braunstein, D.; Doster, W.; Frauenfelder, H.; Hong, M. K.; Johnson, J. B.; Luck, S.; Ormos, P.; Schulte, A.; Steinbach, P. J.; Xie, A. H.; Young, R. D. Glassy Behavior of a Protein. *Phys. Rev. Lett.* **1989**, *62* (16), 1916−1919.
(92) Lubchenko, V.; Wolynes, P. G.; Frauenfelder, H. Mosaic Energy Landscapes of Liquids and the Control of Protein Conformational Dynamics by Glass-Forming Solvents. *J. Phys. Chem. B* **2005**, *109* (15), 7488−7499.
(93) Kuo, Y.-H.; Chiang, Y.-W. Slow Dynamics around a Protein and Its Coupling to Solvent. *ACS Cent. Sci.* **2018**, *4* (5), 645−655.
(94) Lubchenko, V.; Wolynes, P. G. Theory of Structural Glasses and Supercooled Liquids. *Annu. Rev. Phys. Chem.* **2007**, *58* (1), 235−266.
(95) Whittington, A. C.; Larion, M.; Bowler, J. M.; Ramsey, K. M.; Brüschweiler, R.; Miller, B. G. Dual Allosteric Activation Mechanisms in Monomeric Human Glucokinase. *Proc. Natl. Acad. Sci. U.S.A.* **2015**, *112* (37), 11553−11558.
(96) Ernst, J. A.; Clubb, R. T.; Zhou, H.-X.; Gronenborn, A. M.; Clore, G. M. Demonstration of Positionally Disordered Water Within a Protein Hydrophobic Cavity by NMR. *Science* **1995**, *267* (5205), 1813−1817.
(97) Denisov, V. P.; Peters, J.; Hörlein, H. D.; Halle, B. Using Buried Water Molecules to Explore the Energy Landscape of Proteins. *Nat. Struct. Mol. Biol.* **1996**, *3* (6), 505−509.
(98) Beach, H.; Cole, R.; Gill, M. L.; Loria, J. P. Conservation of Ms-ms Enzyme Motions in the Apo- and Substrate-Mimicked State. *J. Am. Chem. Soc.* **2005**, *127* (25), 9167−9176.

https://doi.org/10.1021/jacs.3c12892
J. Am. Chem. Soc. XXXX, XXX, XXX−XXX